OMTN, Volume 27

Supplemental information

SPI1-induced downregulation of FTO promotes GBM progression by regulating pri-miR-10a processing in an m6A-dependent manner

Shouji Zhang, Shulin Zhao, Yanhua Qi, Boyan Li, Huizhi Wang, Ziwen Pan, Hao Xue, Chuandi Jin, Wei Qiu, Zihang Chen, Qindong Guo, Yang Fan, Jianye Xu, Zijie Gao, Shaobo Wang, Xing Guo, Lin Deng, Shilei Ni, Fuzhong Xue, Jian Wang, Rongrong Zhao, and Gang Li

Supplementary Results

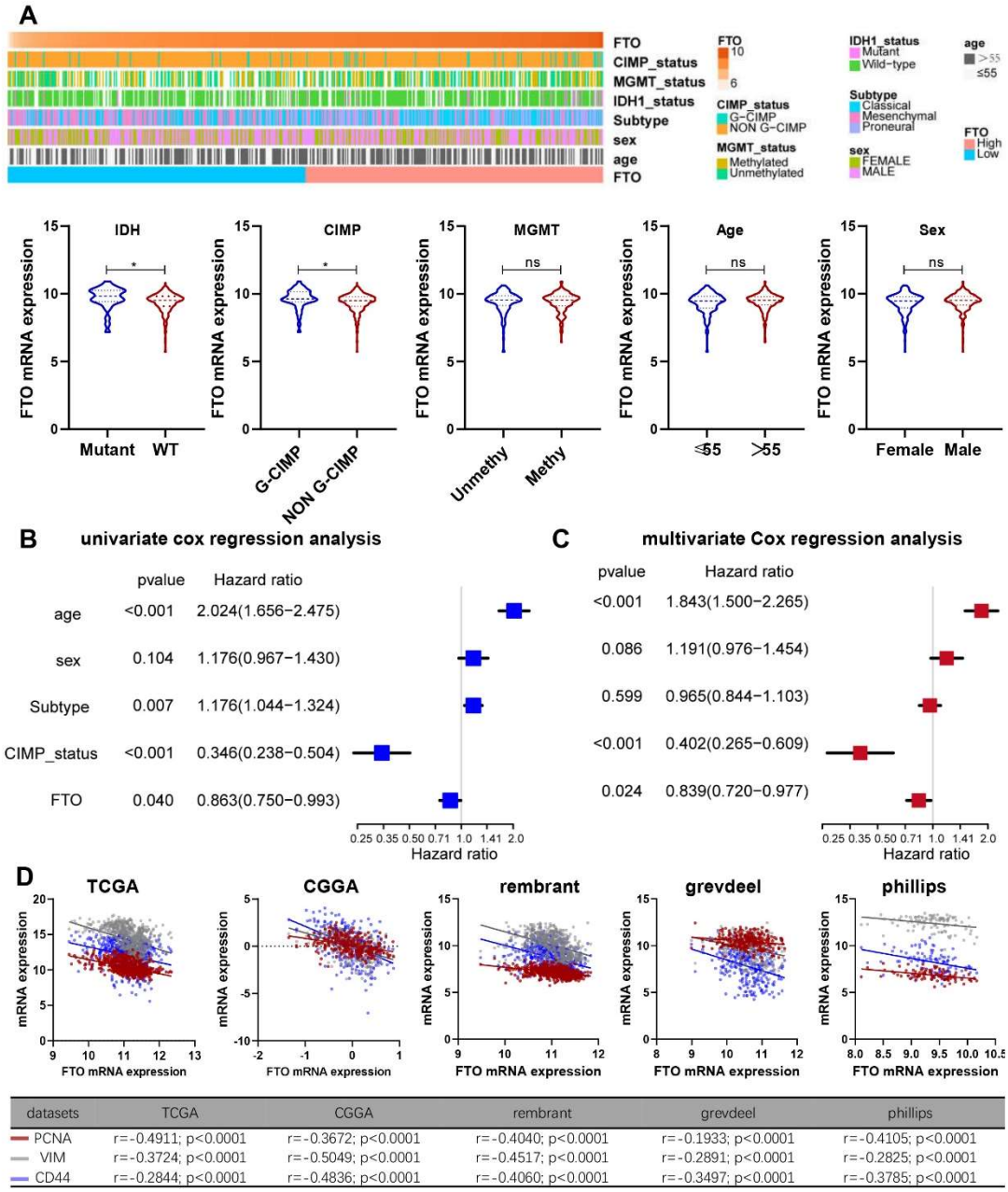

datasets	TCGA	CGGA	rembrant	grevdeel	phillips
PCNA	r=-0.4911; p<0.0001	r=-0.3672; p<0.0001	r=-0.4040; p<0.0001	r=-0.1933; p<0.0001	r=-0.4105; p<0.0001
VIM	r=-0.3724; p<0.0001	r=-0.5049; p<0.0001	r=-0.4517; p<0.0001	r=-0.2891; p<0.0001	r=-0.2825; p<0.0001
CD44	r=-0.2844; p<0.0001	r=-0.4836; p<0.0001	r=-0.4060; p<0.0001	r=-0.3497; p<0.0001	r=-0.3785; p<0.0001

Figure S1. Associations between FTO and GBM clinical features. (A) Distribution of FTO expression in different cohorts stratified by IDH1 status (mutant (Mut), n=29; wild-type (WT), n=370; p=0.0219), G-CIMP status (G-CIMP, n=45; non-G-CIMP, n=477; p=0.0131), MGMT promoter status (methylated, n=167; unmethylated, n=177; p=0.8281), age (high, age > 55, n=311; low, age ≤ 55, n=211; p=0.0984) and sex (female, n=203; male, n=319; p=0.0803). **(B)** Univariate and **(C)** multivariate Cox regression analyses of FTO expression and other clinical features in the overall survival of GBM samples. **(D)** The Pearson correlation between FTO and PCNA, vimentin (VIM) and CD44 in TCGA, CGGA, Rembrandt, Gravendeel and Phillips datasets.

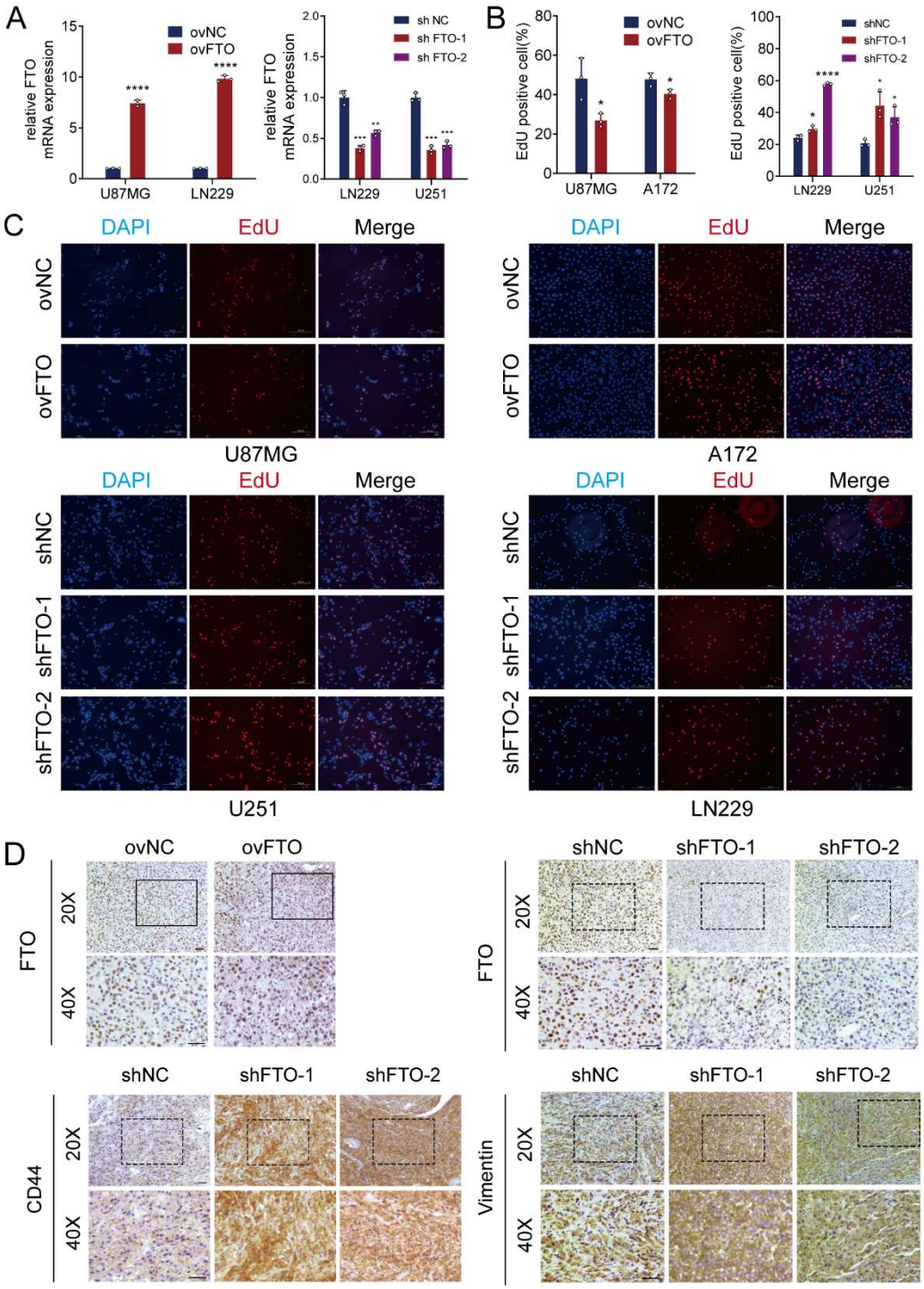

Figure S2. FTO inhibited GBM progression in vitro and in vivo. (A) RNA expression of FTO in GBM cells transfected with lentivirus as indicated. Student's *t* test was used for statistical analysis. **(B, C)** EdU assays of GBM cells transfected with lentivirus as indicated. Student's *t* test was used for statistical analysis. **(D)** IHC of FTO, CD44 and vimentin expression in xenograft sections of nude mice. Scale bar, 50 μm. Error bars indicate at least three independent experiments, and data are shown as the mean ± SD. *p<0.05, **p<0.01, ***p<0.001.

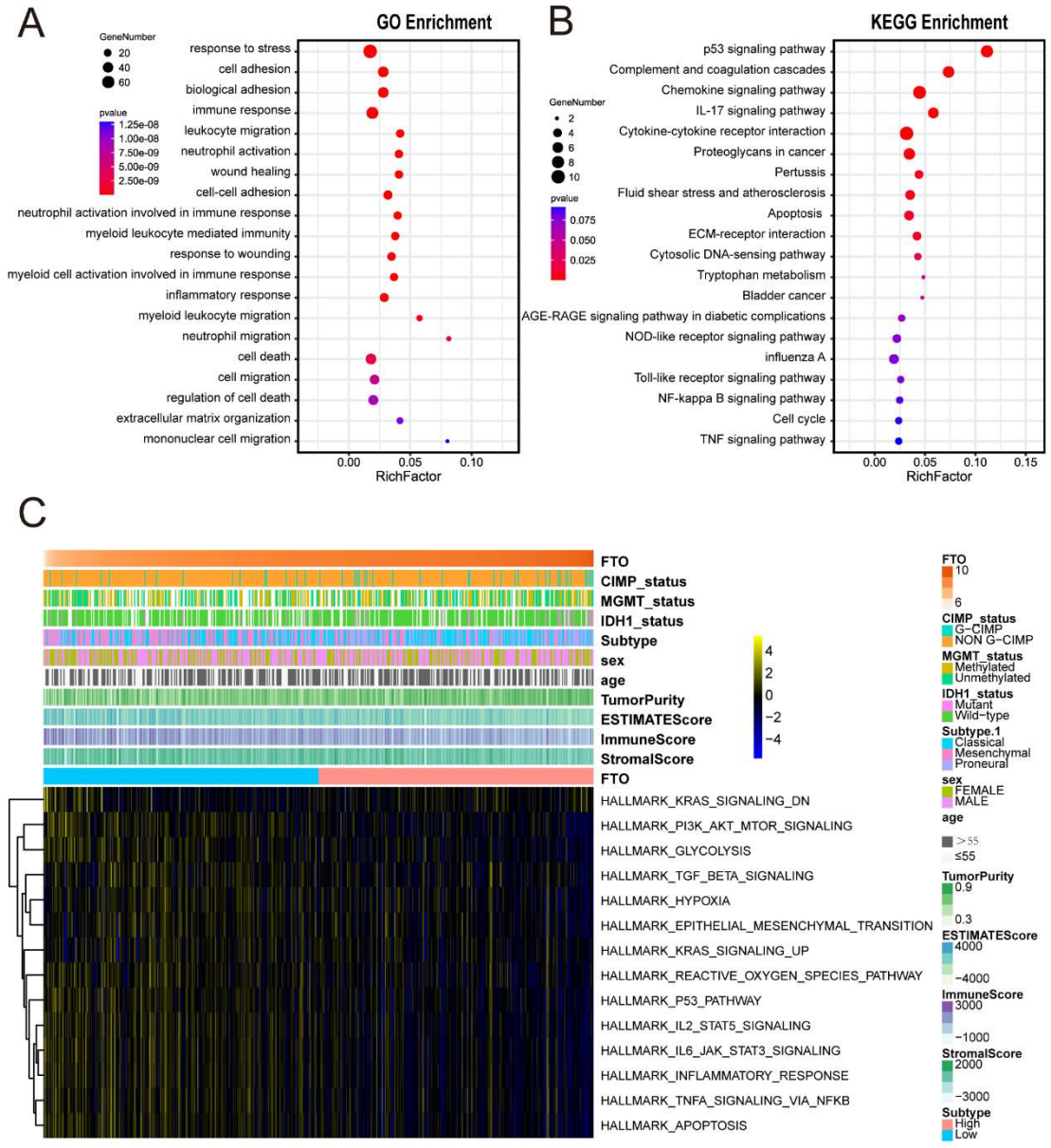

Figure S3. Functional analysis of FTO in the TCGA GBM dataset. (A) Enriched Gene Ontology biological process (GO BP) terms and **(B)** KEGG pathways for the downregulated genes in the FTO high group. **(C)** GSVA enrichment analysis showing the activation status of biological pathways in the FTO high and low expression groups. A heatmap was used to visualize these biological processes; yellow represents activated pathways, black represents median activated pathways and blue represents inhibited pathways.

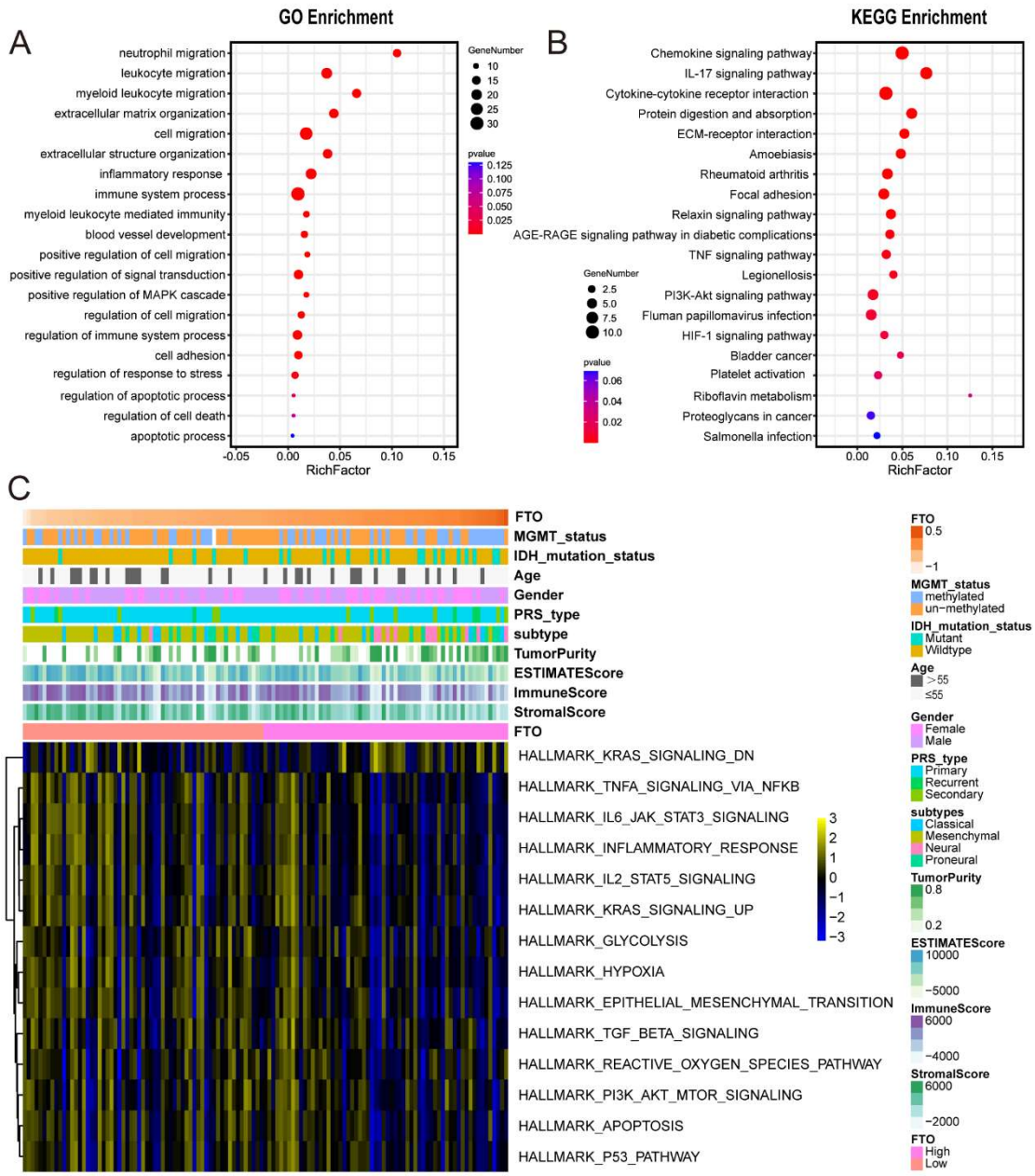

Figure S4. Functional analysis of FTO in the CGGA GBM dataset. (A) Enriched Gene Ontology biological process (GO BP) terms and **(B)** KEGG pathways for the downregulated genes in the FTO high group. **(C)** GSVA enrichment analysis showing the activation status of biological pathways in the FTO high and low expression groups. A heatmap was used to visualize these biological processes; yellow represents activated pathways, black represents median activated pathways and blue represents inhibited pathways.

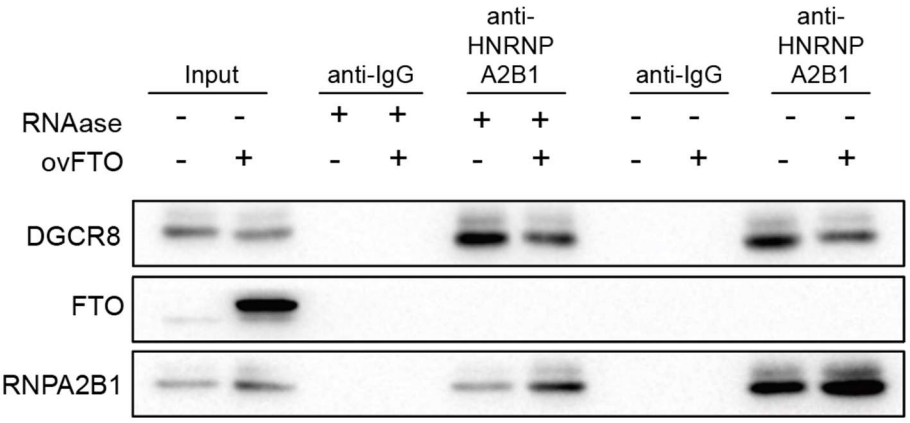

Figure S5. HNRNPA2B1 interacted with the microprocessor independent of RNA. Interaction between DGCR8 and HNRNPA2B1. After immunoprecipitation, samples were washed and incubated with RNase as indicated.

>NC_000017.11:c48580047-48579947 Homo sapiens chromosome 17, GRCh38.p13 Primary Assembly
AAAACTAGAACAAAACGAAATAAAACCAAAGCACTCAAACCACACCCCAAACGAAGAAG
GCGCGGAAAGTAGGA GAACTGGAAAATTTCTGGGCCAAGAAG

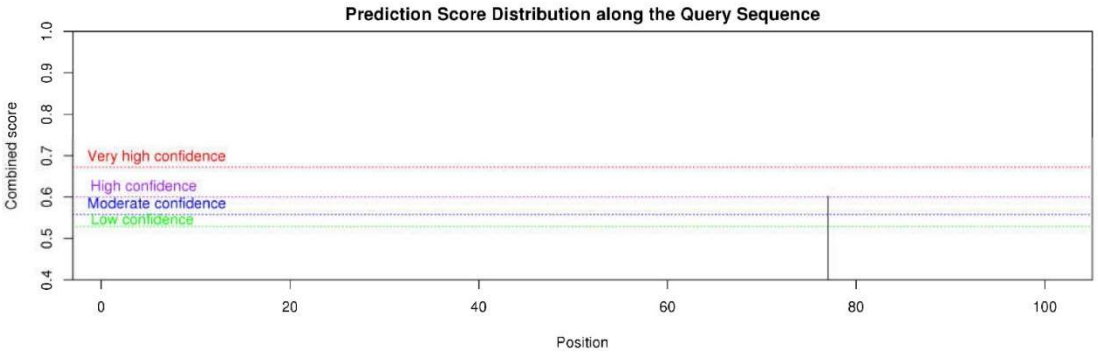

Score(binary)	Score(knn)	Score(spectrum)	Score(combined)	Decision
0.692	0.606	0.479	0.602	m^6A site (**High** confidence)

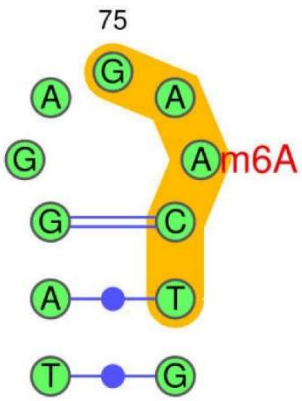

Figure S6. Schematic representation of the reporters was generated to determine the m6A site on pri-miR-10a using the SRAMP (http://www.cuilab.cn/sramp) database. The top reporter contains WT fasta sequences upstream from pre-miR-10a, and the potential sites of methylation are depicted as red dots.

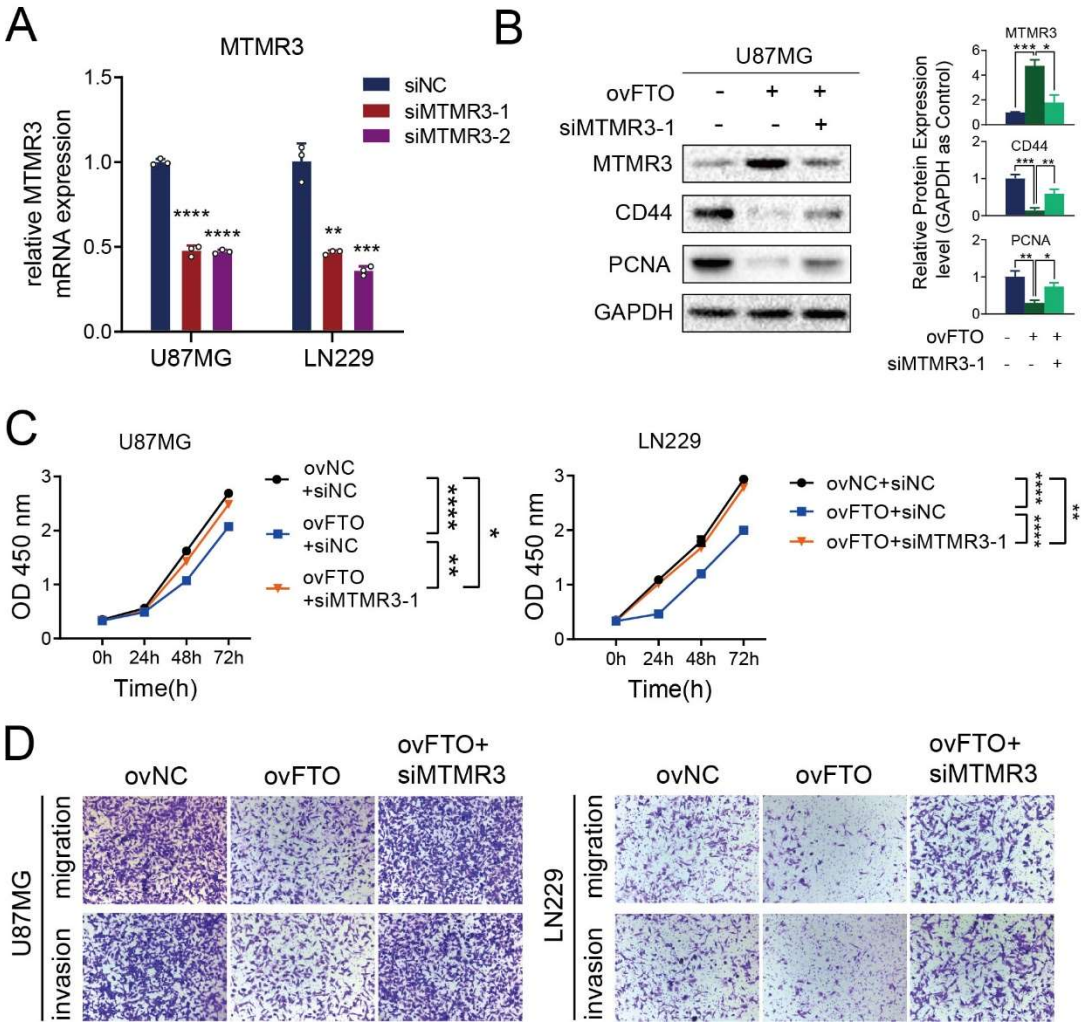

Figure S7. MTMR3 knockdown reversed the inhibition of proliferation, migration and invasion of GBM cells induced by FTO overexpression. (A) The mRNA expression level of MTMR3 in U87MG and LN229 transfected by siNC, siMTMR3-1 or siMTMR3-2. **(B)** Protein expression level of U87MG cells (n=3). (C) CCK-8 assay of U87MG and LN229 cells. **(D)** Transwell assays of U87MG and LN229 cells transfected by siMTMR3-1 as indicated. Statistical analysis was performed by Student's t test. Error bars indicate at least three independent experiments, and data are shown as the mean ± SD. *P<0.05, **P< 0.01, ***P<0.001, ****P<0.0001.

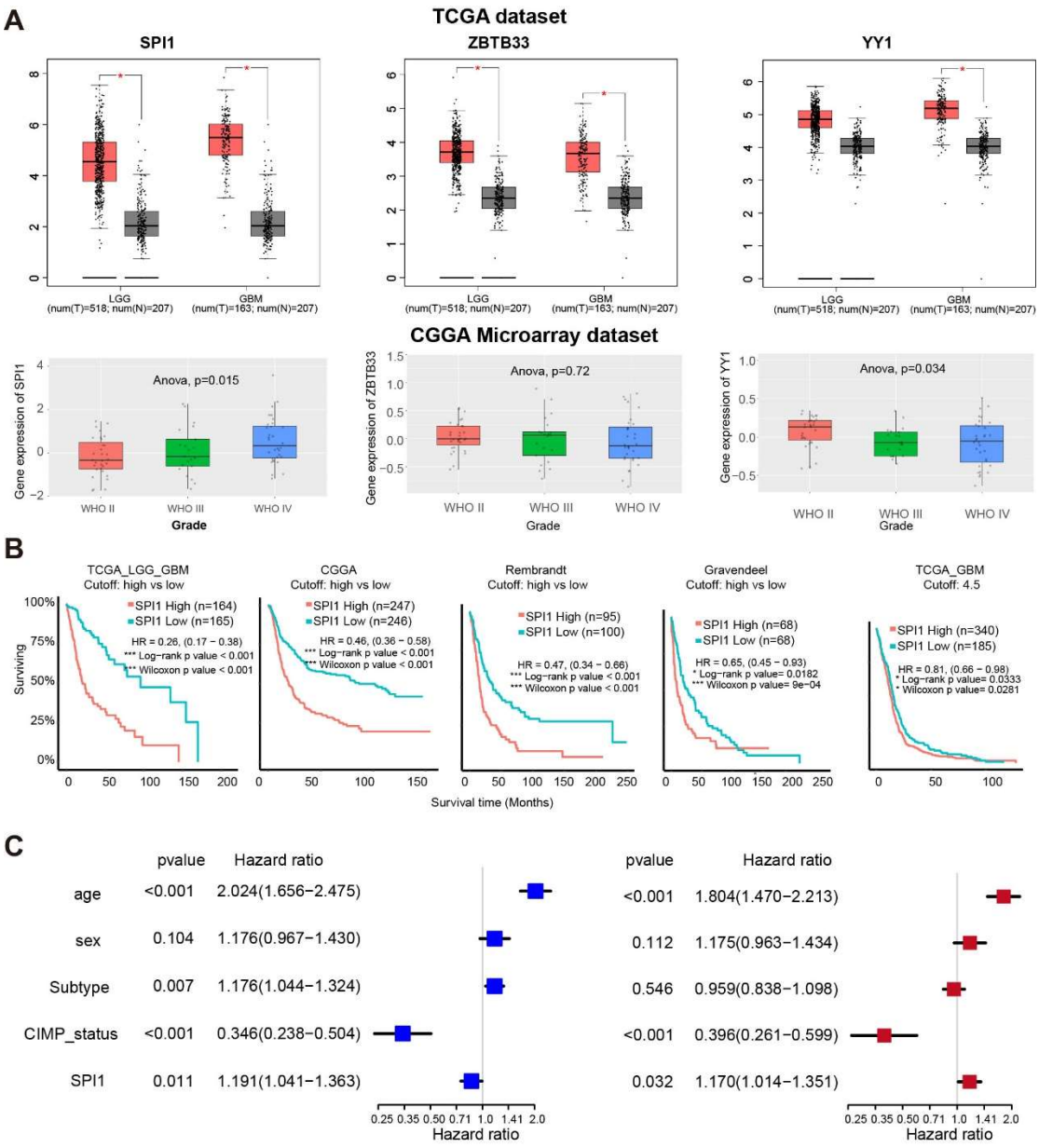

Figure S8. SPI1 expression correlated with poor prognosis of GBM patients. (A) The expression of SPI1, ZBTB33 and YY1 in the TCGA and CGGA microarray datasets. **(B)** Kaplan–Meier survival curves of patients with high and low SPI1 expression in TCGA, CGGA, Rembrandt, Gravendeel and Philips datasets. The log-rank test was used to compare differences between two groups. **(C)** Univariate and multivariate Cox regression analyses of SPI1 expression and other clinical features in the overall survival of TCGA GBM samples.

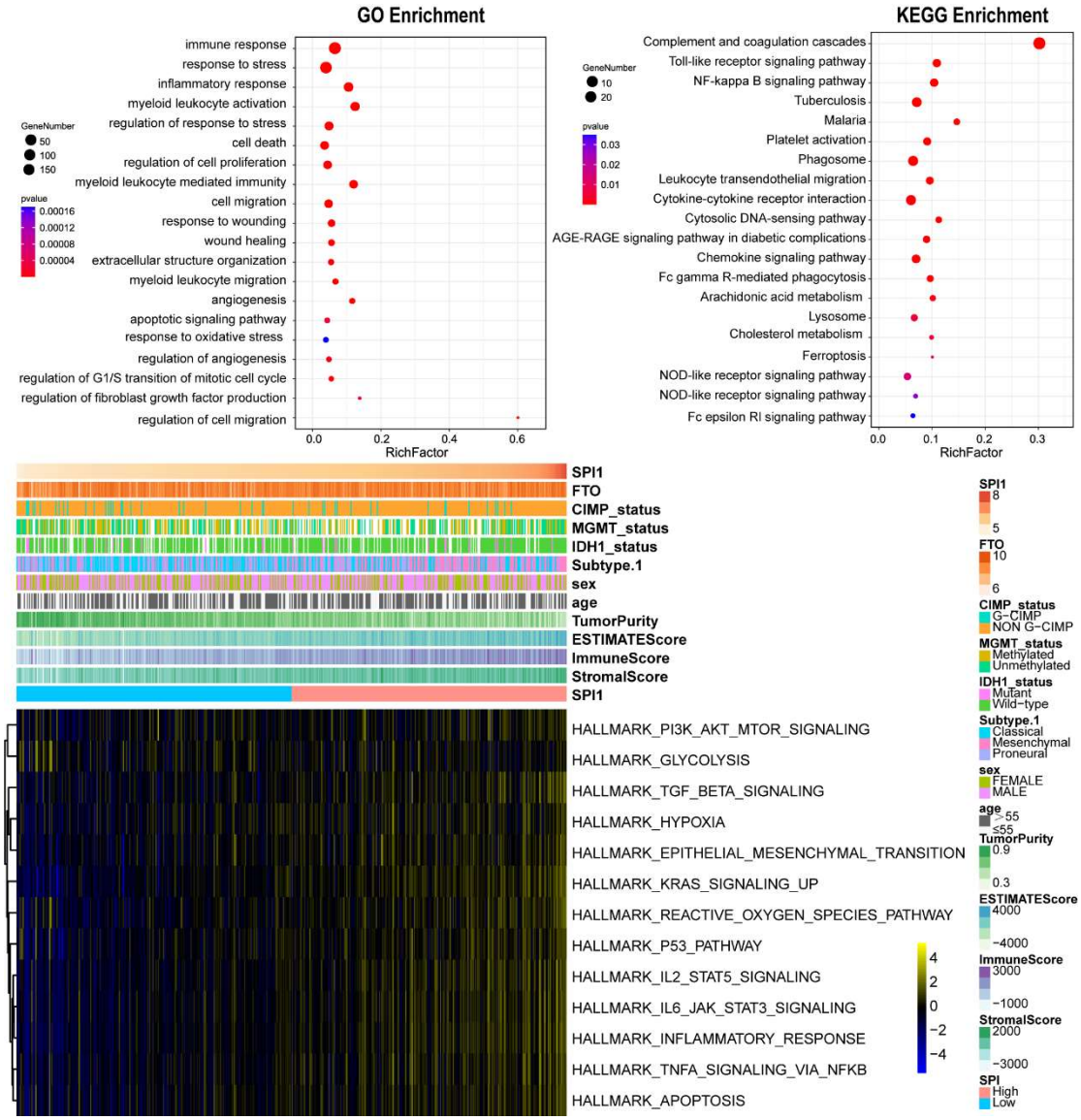

Figure S9. Functional analysis of SPI1 in the TCGA GBM dataset. (A) Enriched Gene Ontology biological process (GO BP) terms and **(B)** KEGG pathways for the downregulated genes in the SPI1 high group. **(C)** GSVA enrichment analysis showing the activation status of biological pathways in the SPI1 high and low expression groups. A heatmap was used to visualize these biological processes; yellow represents activated pathways, black represents median activated pathways and blue represents inhibited pathways.

Figure S10. Functional analysis of SPI1 in the CGGA GBM dataset. (A) Enriched Gene Ontology biological process (GO BP) terms and **(B)** KEGG pathways for the downregulated genes in the SPI1 high group. **(C)** GSVA enrichment analysis showing the activation status of biological pathways in the SPI1 high and low expression groups. A heatmap was used to visualize these biological processes; yellow represents activated pathways, black represents median activated pathways and blue represents inhibited pathways.

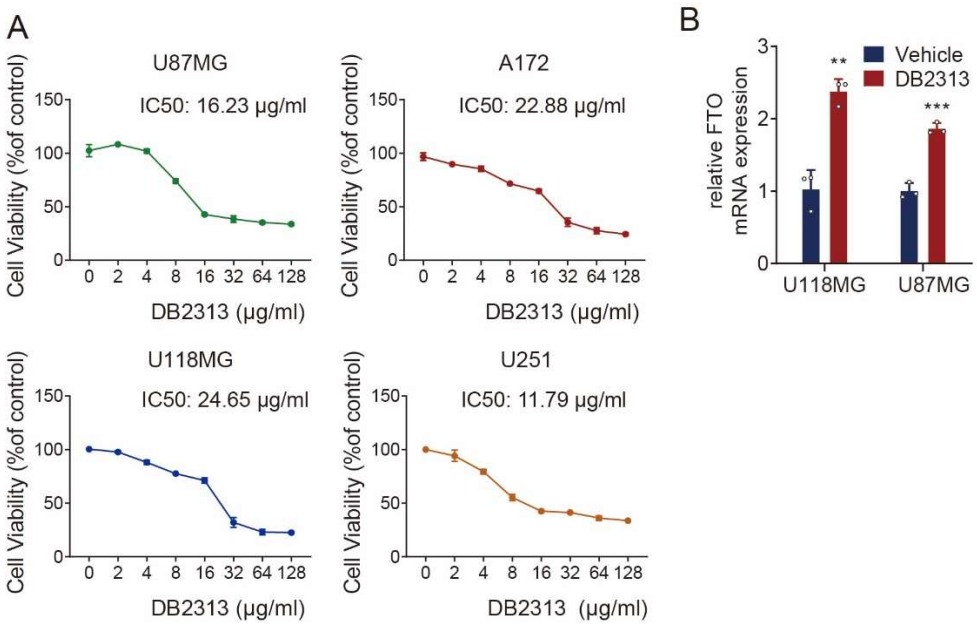

Figure S11. SPI1 inhibited the transcriptional activity of FTO. (A) The IC50 of DB2313 in various GBM cells. **(B)** The relative mRNA expression of FTO in GBM cells treated with DMSO or DB2313. Student's t test was used for statistical analysis. Data are shown as the mean ± SD. **p<0.01, ***p<0.001.

Supplementary Method

Differential expression analysis and functional analysis

Differential expression analysis of miRNAs using RNA sequencing data was performed using the R package "DEseq2", and differential expression analysis of microarray data of TCGA and CGGA GBM datasets was performed using the R package "limma". The differentially regulated genes (|Log2FC|≥1, padj<0.05) were subjected to Gene Ontology (GO) and Kyoto Encyclopedia of Genes and Genomes (KEGG) enrichment analyses. To further explore the biological behaviours among samples with differential FTO and SPI1 expression, we used various HALLMARK gene sets[(1)] from the MSigDB database to estimate pathway enrichment scores for each sample.

Univariate and multivariate Cox regression analyses

We performed univariate and multivariate Cox regression analyses to calculate the hazard ratios (HRs) for FTO and SPI1 and the clinical parameters in the TCGA GBM cohort, and the "forestplot" R package was employed to visualize the data of the Cox regression analysis of FTO and SPI1.

RNA library preparation and sequencing

Total RNA from tissues was isolated by using TRIzol Reagent (Invitrogen) according to the manufacturer's instructions. RNA quality and quantity were assessed using a NanoDrop 2000 spectrophotometer (Thermo Fisher Scientific) and Agilent 2100 Bioanalyzer (Agilent Technologies). Short-chain RNA (miRNA) libraries were prepared by using the NEBNext Multiplex Small RNA Library Prep Set for Illumina®

(NEB) and the NEBNext® UltraTM RNA Library Prep Kit (NEB). miRNA sequencing was performed using the HiSeqX and HiSeq2500 platforms (Illumina) according to the Illumina standard protocol by Beijing Novel Bioinformatics Co., Ltd. (https://en.novogene.com/).

REFERENCES

1. Liberzon, A., Birger, C., Thorvaldsdóttir, H., Ghandi, M., Mesirov, J. and Tamayo, P. (2015) The Molecular Signatures Database (MSigDB) hallmark gene set collection. *Cell systems*, **1**, 417-425.